THE JOURNAL OF PHYSICAL CHEMISTRY B

ARTICLE

pubs.acs.org/JPCB

Theoretical Study of the Mechanism of Proton Transfer in the Esterase Estb from *Burkholderia Gladioli*

Liang Chen,[†,‡,⊥] Xiangqian Kong,[†,⊥] Zhongjie Liang,[†] Fei Ye,[†] Kunqian Yu,[†] Weiyi Dai,[‡] Daocheng Wu,[*,‡] Cheng Luo,[*,†,§] and Hualiang Jiang[†]

[†]Drug Discovery and Design Center, State Key Laboratory of Drug Research, Shanghai Institute of Materia Medica, Chinese Academy of Sciences, Shanghai 201203, China

[‡]The Key Laboratory of Biomedical Information Engineering of the Ministry of Education, School of Life Science and Technology, Xi'an Jiaotong University, Xi'an 710049, China

[§]Center for Systems Biology, Soochow University, Jiangsu 215006, China

Supporting Information

ABSTRACT:

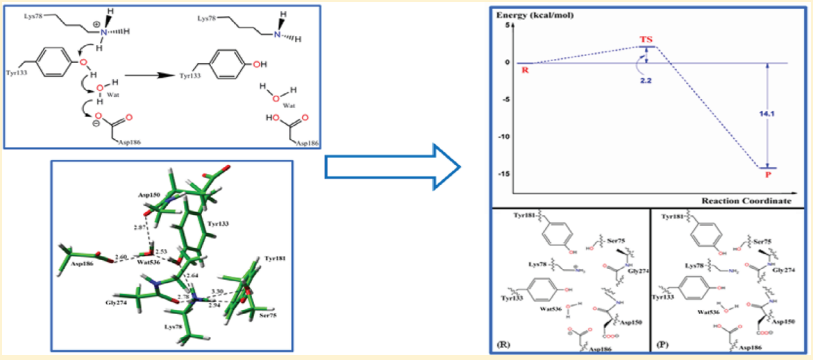

Esterase EstB from *Burkholderia gladioli* belongs to a novel class of esterases homologous to penicillin binding proteins, notably DD-peptidase and class C β-lactamases. It can cleave the side chain acetyl ester group from cephalosporins leaving the β-lactam ring intact, which is a feature of relevance to industrial biocatalytic applications in the production of semisynthetic cephalosporin derivatives. Due to its important role as a potential biocatalyst in industry, the significance of EstB has been greatly appreciated. However, the molecular basis for those residues involving catalysis of EstB remains elusive. By analyzing the crystal structure of EstB, we identified a conserved water molecule in active-site cavity which might mediate an intramolecular proton transfer (PT) from Lys78 to Asp186 via Tyr133. Then a combined computational approach including molecular dynamics (MD) simulations and quantum mechanics/molecular mechanics (QM/MM) calculations was employed to explore this presumable PT mode in the native enzyme. A 30 ns MD simulation of the enzyme highlights the conserved H-bond network involving Lys78, Tyr133, Asp186, and the conserved water molecule in the active site. In particular, the water molecule did not exchange with bulk solvent, indicating its structural and functional relevance. The energy profile calculated by QM/MM approach displayed a notably low PT barrier (2.2 kcal/mol) and a dramatic energy difference (14.1 kcal/mol) in reactants versus immediate products, which implies that the proposed proton shuttle is concerted and energetically favorable. Our studies offer a reasonable pathway to yield a free base by assisting Lys78 deprotonation, thereby paving the way for future studies on Ser75 activation that is a critical step in catalysis by EstB, as well as biocatalyst development by rational attempts. This PT mode would also afford clues for the forthcoming investigation on acyltransferase LovD that is homologous to EstB.

INTRODUCTION

The growing demanding for pharmaceuticals led to numerous new strategies for their industrial production. Apart from transition metal catalysis preferred by organic chemists, biocatalysis by enzymes for drug synthesis also demonstrates a promising future.[1,2] Among these enzymes, EstB, a novel esterase isolated from *Burkholderia gladioli*, is a candidate to serve as such a biocatalyst due to its ability to cleave the side chain acetyl ester group from cephalosporins leaving the β-lactam ring intact, which is a feature of relevance to industrial biocatalytic applications in the production of semisynthetic cephalosporin derivatives.[3] By application of directed evolution, the stability and potency of

Received: July 4, 2011
Revised: September 9, 2011
Published: September 12, 2011

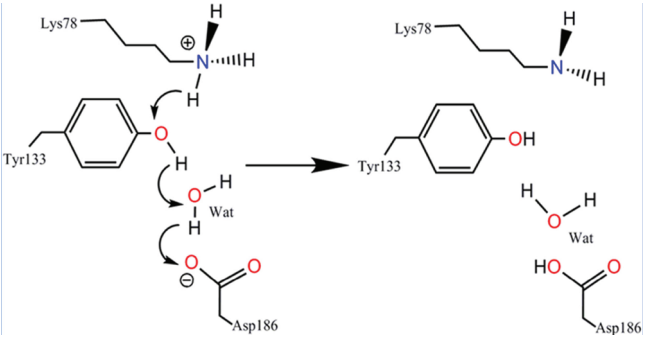

Figure 1. Proposed PT process in EstB.

an esterase EstB variant toward cephalosporins were improved 129-fold compared to wild type.[4]

EstB belongs to a novel class of esterases homologous to penicillin binding proteins, notably DD-peptidase and class C β-lactamases. Specifically, EstB reveals the motif Ser-X-X-Lys, which is the characteristic for β-lactamases in the X-ray crystal structure.[5] Besides, the peptides Tyr-Ser-Leu and Trp-Gly-Gly, equivalent to SDN-loop and KTG-box, respectively, in class C β-lactamases, are also found in this esterase.[5] In parallel, based on a striking similarity of active-site architecture between esterase EstB and class C β-lactamase P99, as well as related experimental data, the serine (Ser75) within the motif Ser-X-X-Lys was believed to act as nucleophile, while several other residues in EstB active-site cavity were reported to be functionally associated.[3,5] However, due to the incomplete knowledge of enzymology concerning esterase EstB (such as the nature and stability of contacts between functional groups that are essential for catalysis), further tailoring of this biocatalyst for other desired properties will be limited, which hence highlights the dire need for an indepth understanding toward its structure/function relationship.

Herein, we further unmasked a potential relationship of several active-site residues by proposing an intramolecular proton transfer (PT) mode via an active-site water molecule: Lys78 → Tyr133 → water → Asp186 (Figure 1). In brief, the trajectory obtained from molecular dynamics (MD) simulation for the fully solvated enzyme emphasizes the stable H-bond network among Lys78, Tyr133, Asp186, and the water molecule, suggesting that a multistep PT event from Lys78 to Asp186 through Tyr133 and the water molecule would occur. Quantum mechanics/molecular mechanics (QM/MM) calculations were next performed to characterize the energy profile of this PT reaction. The calculation results reveal that the proposed proton shuttle is favorable. This presumable PT process in the native EstB offers a reasonable way for the generation of the unprotonated Lys78 that can act as a free base, thereby setting the basis for future exploration on Ser75 activation that is a critical step in catalysis by EstB, as well as biocatalyst development by rational attempts.

MATERIALS AND METHODS

2.1. MD Simulations of the Native Form of the Esterase EstB. Initial coordinates for the protein atoms and the crystallographic water molecules were extracted from the X-ray crystal structure of the esterase EstB at 2.0 Å resolution (PDB code: 1CI8, chain B).[5] The dominant protonation states of ionizable residues were determined at constant pH = 7 by using the Poisson–Boltzmann method via the H++ program.[6] The protein atoms, as well as all the water molecules of the crystal structure, were solvated into a rectangular box with a 10 Å buffer distance between the solvent box wall and the nearest solute atoms. Afterward, counterions were added to the system to neutralize the simulation system, and finally, the whole system was subjected to energy minimization.

All MD simulations were performed using the AMBER package (version 10.0)[7] with constant temperature and pressure (NPT) and periodic boundary conditions. The Amber99SB[8−10] force field for the protein and TIP3P model[11] for water molecules were employed. During MD simulations, all the bonds involving hydrogen atoms were constrained with the SHAKE algorithm,[12] and the integration step of 2 fs was used. Electrostatic interactions were calculated using the particle-mesh Ewald method.[13] The nonbonded cutoff was set to 10.0 Å, and the nonbonded pairs were updated every 25 steps. The simulation was coupled to a 300 K thermal bath at 1.0 atm of pressure (atm = 101.3 kPa) by applying the algorithm of Berendsen et al.[14] The temperature and pressure coupling parameters were set as 1 ps.

2.2. QM/MM Calculations. QM/MM calculations were performed with the use of a two-layered ONIOM scheme encoded in the Gaussian03 program.[15] The ONIOM method is a hybrid computational approach developed by Morokuma and co-workers that allows different levels of theory to be applied to different parts of a molecular system.[16−21] In this approach, the molecular system under investigation is defined as two parts. The "model" system consists of the most critical elements of the system and is treated with an accurate (high-level) computational method which can describe bond breaking and formation. The "real" system includes the entire system and is treated with an inexpensive (low-level) computational method which can depict the environmental effects of the molecular environment on the model system. The total ONIOM energy, E_{ONIOM}, is defined as the following

$$E_{\mathrm{ONIOM}} = E_{(\mathrm{high,\,model})} + E_{(\mathrm{low,\,real})} - E_{(\mathrm{low,\,model})}$$

where $E_{(\mathrm{high,\ model})}$ is the energy of the model system (includes the link atoms) at the high level of theory, $E_{(\mathrm{low,\ real})}$ is the energy of the real system at the low level of theory, and $E_{(\mathrm{low,\ model})}$ is the energy of the model system at the low level of theory. Thus, the ONIOM method allows one to perform a high-level calculation on just a small, critical part of the molecular system and incorporate the effects of the surrounding elements at a lower level of theory to yield a consistent energy expression on the full system.

A representative snapshot from MD simulation provided initial coordinates for the QM/MM calculations, and all water molecules within 20 Å of the Ser75 were kept. The QM region consists of the side chains of Lys78, Tyr133, and Asp186 (the proton shuttling residues); the side chains of Ser75 and Tyr181, the backbone atoms of Gly274, as well as the entire Asp150; and the water molecule (Wat536) in the active site. The link hydrogen atoms were employed to saturate the dangling covalent bonds in the QM region. The atoms in QM region amount in the aggregate to 91 and were optimized using the density functional theory with the B3LYP exchange-correlation functional and 6-31G* basis set. The remainder of the system (MM region) was treated by using the AMBER Parm99 force field. A total of 5719 atoms were included for the QM/MM calculations. The potential energy profile was constructed by incrementing the reaction coordinates by a fixed value (0.05 Å), followed by a geometry optimization at the B3LYP/6-31G*.

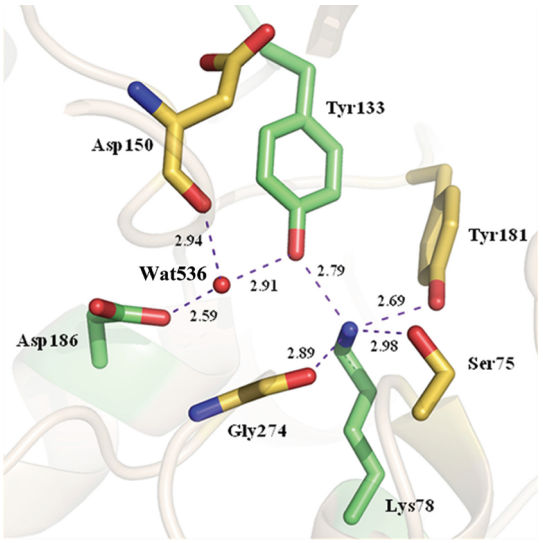

Figure 2. Stereoview of the hydrogen bonding network surrounding Wat536 inside EstB active site (PDB code: 1CI8, chain B).

Table 1. Predicted pK_a for Ionizable Residues in Three Distinct States with Different Internal Dielectric Constants

	pK_a				
ε_{in}[a]	Tyr181	Lys78	Tyr133	Asp186	Asp150
4	11.3	>14	>14	<0	<0
6	10.3	>14	>14	<0	<0
10	9.9	>14	>14	<0	<0

[a] Internal dielectric constants.

RESULTS AND DISCUSSION

3.1. Reidentification of X-ray Crystallographic Data. The X-ray crystallographic structures of native EstB and its complex with diisopropyl fluorophosphate (DFP) were determined about one decade ago.[5] Previous biochemical and structural studies have suggested that Ser75 acts as the catalytic nucleophile, while Lys78 and Tyr181 may contribute to Ser75 activation in the reaction.[3,5] In an effort to gain deeper insight into the potential functional groups that are essential for catalysis, we reanalyzed the X-ray crystallographic structures of EstB. In the catalytic cavity of native EstB (PDB code: 1CI8, chain A and chain B),[5] the side chain of lysine residue (Lys78) interacts with the Ser75 (Lys78 N_ζ...O_γ Ser75, 2.7−3.0 Å), Tyr181 (Lys78 N_ζ...O_η Tyr181, 2.6−2.9 Å), Gly274 (Lys78 N_ζ...O Gly274, 2.8−3.0 Å), and Tyr133 (Lys78 N_ζ...O_η Tyr133, 2.7−2.8 Å). An intriguing phenomenon is the following: Tyr133, through a water molecule (Wat536), contacts the carboxylate group of the Asp186 (which is on an α-helix). Meanwhile, this water molecule contacts the backbone carbonyl group of Asp150 and thus seemingly is stabilized by an extensive H-bond network (Figure 2). We further checked the B factor of the water oxygen atom and found it is lower than the average B factor for all residues and waters, confirming that this water molecule is much less flexible. On the other hand, due to the fact that a water molecule with a relatively low B factor was also found at the similar position between the side chains of a tyrosine and an aspartic acid in the acyltransferase LovD that is homologous to EstB (as discussed below), the water molecule located in such a position seems to be structurally conserved in esterase EstB versus acyltransferase LovD.

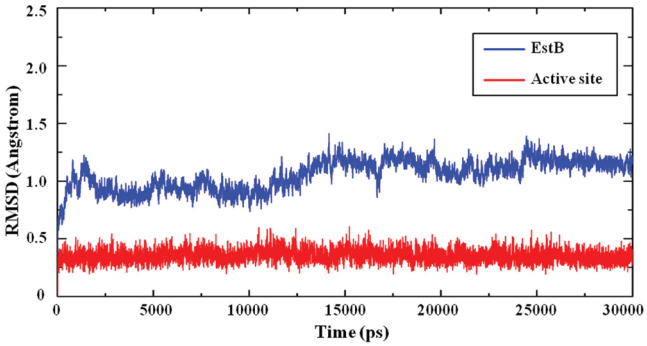

Figure 3. Time dependencies of the weighted root-mean-square deviations for the backbone atoms of EstB and active-site residues (Ser75, Lys78, Tyr133, Asp150, Tyr181, Asp186, Gly274) from their initial positions during the 30 ns simulation.

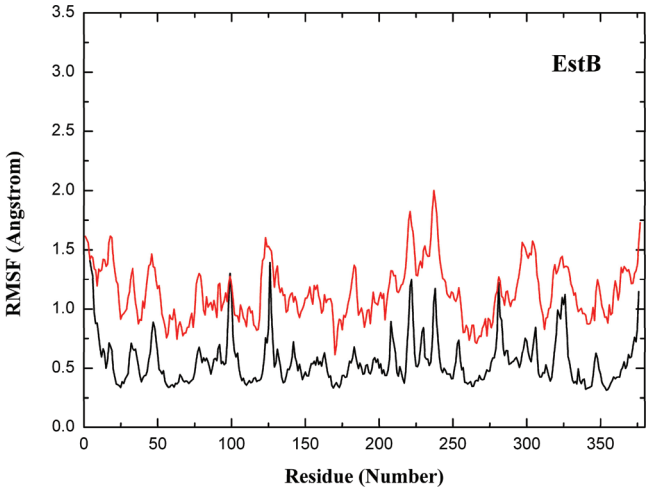

Figure 4. Residue fluctuations obtained by averaging residual fluctuations over the MD simulation (black curve) and by computing the value from experimentally derived B factors (red curve) for the EstB crystal structure.

To date, intramolecular PT reactions via conserved active-site water molecules have been recognized in many biological systems. Typical examples include green fluorescent protein and class A β-lactamases.[22−24] Similarly, due to the appearance of general PT donor (Lys78) and acceptor (Asp186), as well as the arrangement of these residues (Lys78, Tyr133, and Asp186) and the water molecule (bridging the two side chains of Tyr133 and Asp186), it is tempting to speculate that a multistep proton shuttle from Lys78 to Asp186 through Tyr133 and the water molecule is allowed inside the EstB active-site cavity.

3.2. Dominant Protonation States of Ionizable Residues at the Active Site. Prior to MD simulation, the acid dissociation constants (pK_a) of ionizable residues were predicted on the basis of native EstB (PDB code 1CI8, chain B)[5] (see Materials and Methods) by using different internal dielectric constants. As illustrated in Table 1, all of the ionizable residues at the active site, including Lys78, Tyr133, Asp150, Tyr181, and Asp186, are with normal protonation states at physiological condition (pH = 7.0).

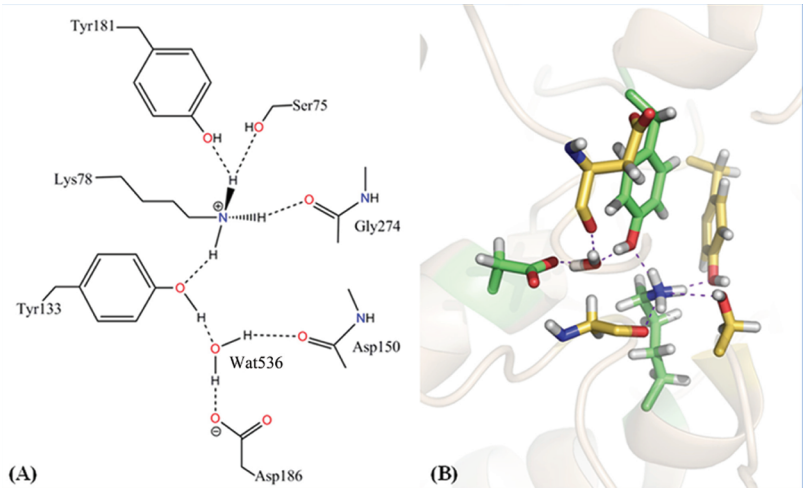

Figure 5. (A) Schematic representation of the most stable H-bond contacts surrounding Wat536. (B) Stereoview of a representative snapshot from MD simulations.

Table 2. Summary of the Average Distance between Heavy Atoms (Å) and Percent Occurrence Data for Important Hydrogen Bonding Interactions

H-bond	X...Y	%
Ser75—O_γ...H—N_ζ—Lys78	2.91	84.0
Tyr181—O_η...H—N_ζ—Lys78	3.08	75.8
Gly274—C═O...H—N_ζ—Lys78	2.85	99.8
Tyr133—O_η...H—N_ζ—Lys78	2.94	98.4
Wat536—O...H—O_η—Tyr133	2.75	99.8
Asp186—$O_{\delta 1}$...H—O—Wat536	2.72	99.5
Asp150—C═O...H—O—Wat536	2.83	94.7

Further analysis indicated that the electrostatic microenvironment inside EstB active site (with one lysine surrounding the tyrosine, Tyr181) is weaker compared with that in class C β-lactamases (with two lysines surrounding the corresponding tyrosine, Tyr150). Thus, the phenolate state is likely to be unstable for the Tyr181 in EstB based on early reports that the phenoxide located in such a position needs to be stabilized by two positively charged lysines (as is the case in class C β-lactamases).[25,26] Furthermore, most recent studies on class C β-lactamases, including ^{13}C NMR titration experiments and an ultrahigh resolution complex structure, have suggested Tyr150 (corresponding to Tyr181 in EstB) is neutral in the apoenzyme and most likely so throughout the reaction,[27,28] thereby providing indirect support for the protonated state of Tyr181 in the native EstB. Taken together, a stable neutral Tyr181 in the apostate of EstB was favored, and all the active-site residues, accordingly, were kept with normal protonation states during the following MD simulation and QM/MM calculation.

3.3. Molecular Dynamics Simulation of EstB in the Native Form. To investigate the stability of the H-bond network surrounding the water molecule in the active site, a 30 ns MD simulation was performed on the EstB in its native form. The temporal development of the weighted root-mean-square deviations (rmsd) for the heavy atoms of backbone of the enzyme from their initial positions (t = 0) were monitored. As illustrated in Figure 3, the steady rmsd for backbone atoms shows that the

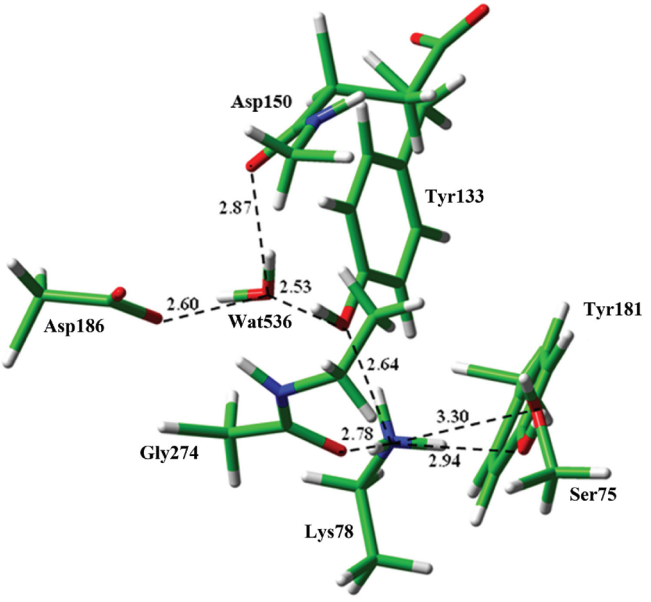

Figure 6. QM region used in this work. The structure displayed here is extracted from MD simulations and then optimized by QM/MM approach.

structural changes in the protein during the course of the MD simulations were moderate, while the flat tendency of the rmsd for the active-site residues indicated that the microenvironment around this water molecule was relatively stable, which was indispensable to the potential PT reaction. Besides, based on the fit of backbone atoms of the active-site residues, the rmsd value of the active-site water molecule (Wat536) was, on average, ~0.6 Å, suggesting a relatively stable Wat536 in the simulation (Figure S1) Meanwhile, the root-mean-square fluctuations (rmsf) (Figure 4), which represents average displacement of residues along the whole simulation process, exhibit consistency between the theoretical value and the calculated value from experimentally derived B factors, signifying that the MD simulation on EstB is reasonable.

To probe molecular basis for the potential PT reaction, the corresponding H-bond interactions in the active site were analyzed.

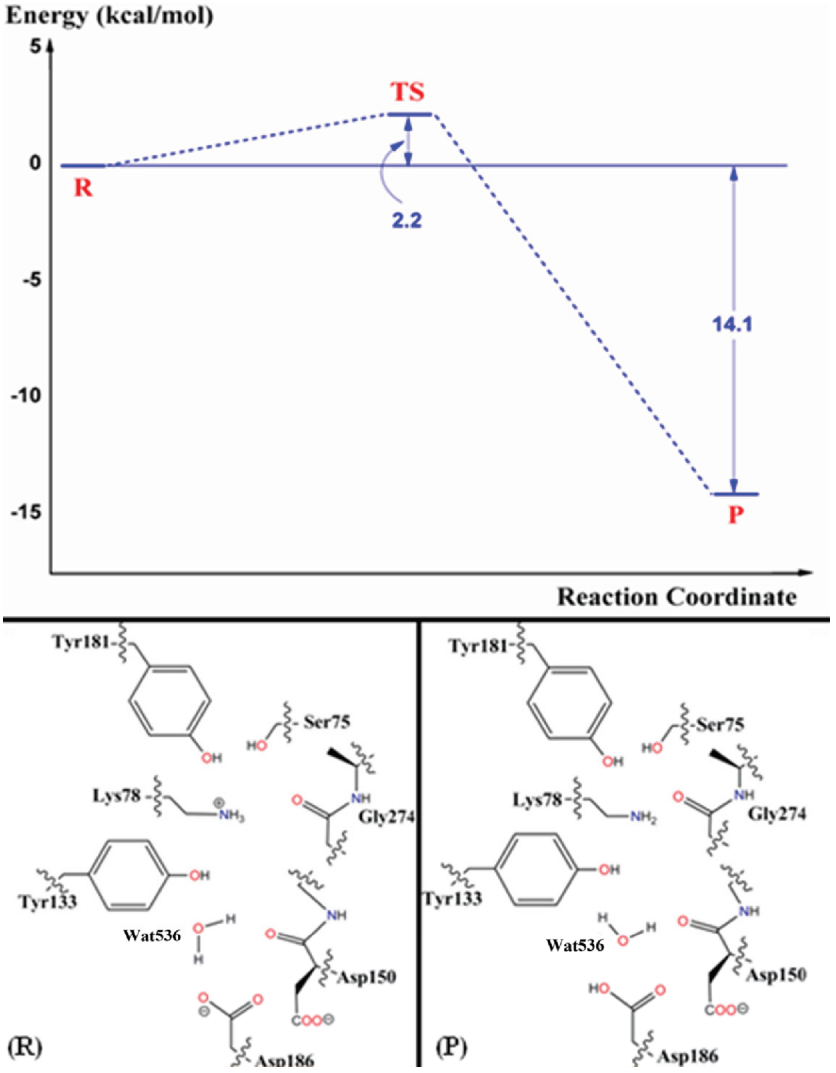

Figure 7. Potential energy profile for the PT reaction. (R) is the reactant; (P) is the immediate product.

Figure 5 shows the schematic representations of the most stable H-bond contacts as well as a representative snapshot extracted from the MD simulation. In Table 2, we collected the average values for the most significant active-site interatomic distances and related H-bond occupancy. As expected, the water molecule was stabilized by the H-bonds with surrounding residues and did not exchange with bulk solvent, showing agreement with a relatively low B factor of the water oxygen from X-ray crystallographic data. In particular, a Wat536 $O_{\zeta}H...O_{\delta 1}$ Asp186 H-bond contact and a Wat536 $O...HO_{\eta}$ Tyr133 H-bond contact were stable along the whole trajectory. The water was also H-bonded with Asp150 by interacting with its backbone carbonyl group intimately. Meanwhile, a stable Lys78 $N_{\zeta}H...O_{\eta}$ Tyr133 H-bond contact was present in the MD trajectory. This stable H-bond network, which is consistent with that in the initial X-ray structure, augments the possibility that the PT event (Lys78 → Tyr133 → water → Asp186) could be triggered. On the other hand, the relatively stable H-bonds among Lys78 and surrounding residues, including Ser75, Tyr181, and Gly274, were also observed in the simulation.

3.4. QM/MM Results. To further explore whether the implied multistep PT process can take place in the catalytic cavity, the QM/MM approach was performed on EstB. From the rmsd analysis in MD simulation shown in Figure 3, the curve approximately from 25 to 30 ns is relatively flat, and thus a snapshot near the middle point in this plateau region of trajectory was extracted and treated as the starting point for the subsequent QM/MM study. As shown in Figure 5, the interaction analysis based on the snapshot indicates that the network of H-bond involving the water molecule (Wat536) and binding site residues (Ser75, Lys78, Tyr133, Asp150, Tyr181, Asp186, and Gly274) closely resembles that observed from X-ray crystal structure (PDB code: 1CI8),[5] confirming this snapshot was a reasonable initial structure for the QM/MM study.

In the QM/MM simulation, the QM region was comprised not only of the active-site water molecule (Wat536) and the side chains of Lys78, Tyr133, and Asp186, but also of the side chains of Ser75 and Tyr181, the backbone atoms of Gly274, and the entire Asp150 (Figure 6). The remainder of the system was included in the MM region. The partitioning scheme for QM and MM regions is described in the Materials and Methods section. We designate this structure as a reactant system. ONIOM, a QM/MM method encoded in Gaussion03, was performed for all the QM/MM calculations.

When systematically lengthening (at 0.05 Å intervals) the O−H bond of the bridging water oriented toward Asp186 by subjecting each step to a geometry optimization, the protons in the hydroxyl group of Tyr133 and ammonium groups of Lys78 migrated in concerted manner. As a consequence, the water proton was bound to Asp186, and meanwhile the other two protons were abstracted by oxygen atom of the water and O_η atom of Tyr133, respectively, giving a protonated Asp186, neutral Tyr133, and free-base Lys78 ensemble. A potential energy profile captured the concerted nature of the PT reaction (Figure 7): the proton movement has a barrier of 2.2 kcal/mol, while the resulting species is 14.1 kcal/mol lower in energy than the reactant species. This energy profile displays a notably low PT barrier and a dramatic energy difference in reactants versus immediate products, which thus prompts us to infer that such a single-direction proton shuttle in the native enzyme is energetically inescapable, or even intrinsic. The corresponding stationary points of potential energy along the PT pathway are shown in Figure S2.

Previous research has proposed that Ser75 acts as the catalytic nucleophile, while Lys78 and Tyr181 may activate Ser75 in the reaction.[3,5] Thus, a critical step of catalysis by EstB is how the Lys78-Tyr181 pair assists Ser75 deprotonation. Our studies on the multistep PT mode in native EstB will provide an implication to this question that Lys78 acts as a general base to activate the catalysis. Meanwhile, given that X-ray crystal structure of EstB-DFP complex (PDB code: 1CI9) (which can be considered as an analogue of the tetrahedral intermediate formed as a result of the nucleophilic attack by the enzyme on the substrate's carbonyl group) reveals a water molecule with a relatively low B factor located in the similar position, as well as a corresponding network of H-bond involving Lys78, Tyr133, water, and Asp186 (shown in Figure S3),[5] it is thus likely that this H-bond network embedded in the catalytic cavity is stable throughout the reaction, which further affords a structural basis for the hypothesis that Lys78 serves as a catalytic base.

3.5. Structural Similarity to Acyltransferase LovD from *Aspergillus terreus*. The acyltransferase LovD from *A. terreus*, a prime biocatalyst for statin drug synthesis, is homologous to esterase EstB (sharing 26% sequence identity). Structural comparison between these two enzymes reveals an extreme similarity of active-site architecture. Aside from the conserved catalytic triad (Ser76-Lys79-Tyr188), the structure of LovD also shows a phenylalanine (Phe363) (which is a counterpart to Trp348 in EstB), as well as a tyrosine (Tyr146) and an aspartic acid (Asp193) at the corresponding position of Tyr133 and Asp186, respectively, in EstB. Interestingly, a water molecule with a relatively low B factor located in the similar position close to the hydroxyl group of tyrosine (Tyr146) and the carboxyl group of aspartic (Asp193) was identified in the cocrystal structures of enzyme with substrate or product (PDB code: 3HLD, 3HLF, 3HLG),[29] and meanwhile it seems to be stabilized by the side chain carbonyl group of a glutamine (Gln270) (Figure S4).[29] As a consequence, the conserved H-bond network involving Lys79, Tyr146, the water molecule, and Asp193 found in LovD, which structurally resembles that in EstB, is also likely to be functionally associated.

CONCLUSIONS

As aforementioned, esterase EstB serves as a potential biocatalyst for industrial production of semisynthetic cephalosporin derivatives, whereas the functional significance of the complex ensemble of residues in the enzyme active site has not been fully unveiled. Therefore, in the present study, we probed the structure/function relationship of EstB with the state-of-art computational methods and theoretically described a PT event via an active-site water molecule in the native EstB. First, by modeling the 3D structure of EstB with theoretical titration methods and MD simulations, we carefully explore the interaction network inside the catalytic cavity. The data from the 30 ns MD simulation afforded insights into an intriguing network of H-bond involving Lys78, Tyr133, the water molecule, and Asp186, while the relative orientation of each H-bond structurally implies that a PT event can be triggered. Second, by QM/MM calculations, we validate such a potential PT process from an energetic standpoint. The energy profile displays a low PT barrier and a dramatic energy difference in reactant versus immediate product and thus suggests that the concerted proton transfer from Lys78 to Asp186 via Tyr133 and the water molecule is inescapable. Taken together, our research provides insights into a significant interresidue relationship inside EstB active-site cavity, hence implicating new avenues for future exploration toward its catalytic mechanism as well as biocatalyst development. In parallel, due to the fact that the active-site architecture of acyltransferase LovD exhibits an extreme structural similarity to that of esterase EstB (including a similar water molecule observed in the cocrystal structures), our studies on EstB would also indirectly contribute to the forthcoming investigation on acyltransferase LovD.

ASSOCIATED CONTENT

Supporting Information. Additional information as noted in the text. This material is available free of charge via the Internet at http://pubs.acs.org.

AUTHOR INFORMATION

Corresponding Author

*Tel. +86-21-50271399; fax +86-21-50807188; e-mail wudaocheng@mail.xjtu.edu.cn (D.W.), cluo@mail.shcnc.ac.cn (C.L.).

Author Contributions

⊥These authors contributed equally to this work.

ACKNOWLEDGMENT

We gratefully acknowledge financial support from the State Key Program of Basic Research of China grant ("973" Program) (2009CB918502 and 2010CB732603), the National Natural Science Foundation of China grants (20972174, 21021063, 30970712, and 91029704), the State Key Laboratory of Drug Research grant (SIMM1105KF-02), the Shanghai Committee of Science and Technology grant (10410703900), and the Special Grant from Chinese Academy of Sciences (XDA01040305).

REFERENCES

(1) Woodley, J. M. *Trends Biotechnol.* **2008**, *26*, 321.
(2) Zhou, H.; Xie, X. K.; Tang, Y. *Curr. Opin. Biotechnol.* **2008**, *19*, 590.
(3) Petersen, E. I.; Valinger, G.; Solkner, B.; Stubenrauch, G.; Schwab, H. *J. Biotechnol.* **2001**, *89*, 11.
(4) Valinger, G.; Hermann, M.; Wagner, U. G.; Schwab, H. *J. Biotechnol.* **2007**, *129*, 98.

(5) Wagner, U. G.; Petersen, E. I.; Schwab, H.; Kratky, C. *Protein Sci.* **2002**, *11*, 467.
(6) Gordon, J. C.; Myers, J. B.; Folta, T.; Shoja, V.; Heath, L. S.; Onufriev, A. *Nucleic Acids Res.* **2005**, *33*, W368.
(7) Case, D. A.; Cheatham, T. E.; Darden, T.; Gohlke, H.; Luo, R.; Merz, K. M.; Onufriev, A.; Simmerling, C.; Wang, B.; Woods, R. J. *J. Comput. Chem.* **2005**, *26*, 1668.
(8) Cornell, W. D.; Cieplak, P.; Bayly, C. I.; Gould, I. R.; Merz, K. M.; Ferguson, D. M.; Spellmeyer, D. C.; Fox, T.; Caldwell, J. W.; Kollman, P. A. *J. Am. Chem. Soc.* **1996**, *118*, 2309.
(9) Wang, J. M.; Cieplak, P.; Kollman, P. A. *J. Comput. Chem.* **2000**, *21*, 1049.
(10) Hornak, V.; Abel, R.; Okur, A.; Strockbine, B.; Roitberg, A.; Simmerling, C. *Proteins* **2006**, *65*, 712.
(11) Jorgensen, W. L.; Chandrasekhar, J.; Madura, J. D.; Impey, R. W.; Klein, M. L. *J. Chem. Phys.* **1983**, *79*, 926.
(12) Ryckaert, J. P.; Ciccotti, G.; Berendsen, H. J. C. *J. Comput. Phys.* **1977**, *23*, 327.
(13) Darden, T.; York, D.; Pedersen, L. *J. Chem. Phys.* **1993**, *98*, 10089.
(14) Berendsen, H. J. C.; Postma, J. P. M.; Vangunsteren, W. F.; Dinola, A.; Haak, J. R. *J. Chem. Phys.* **1984**, *81*, 3684.
(15) Frisch, M. J.; et al. *Gaussian 03*, revision B.05; Gaussian, Inc.: Pittsburgh, PA; 2003.
(16) Maseras, F.; Morokuma, K. *J. Comput. Chem.* **1995**, *16*, 1170.
(17) Svensson, M.; Humbel, S.; Morokuma, K. *J. Chem. Phys.* **1996**, *105*, 3654.
(18) Dapprich, S.; Komaromi, I.; Byun, K. S.; Morokuma, K.; Frisch, M. J. *J. Mol. Struct. THEOCHEM* **1999**, *462*, 1.
(19) Vreven, T.; Morokuma, K. *J. Comput. Chem.* **2000**, *21*, 1419.
(20) Vreven, T.; Mennucci, B.; da Silva, C. O.; Morokuma, K.; Tomasi, J. *J. Chem. Phys.* **2001**, *115*, 62.
(21) Vreven, T.; Morokuma, K.; Farkas, O.; Schlegel, H. B.; Frisch, M. J. *J. Comput. Chem.* **2003**, *24*, 760.
(22) Lill, M. A.; Helms, V. *Proc. Natl. Acad. Sci. U.S.A.* **2002**, *99*, 2778.
(23) Zhang, R. B.; Nguyen, M. T.; Ceulemans, A. *Chem. Phys. Lett.* **2005**, *404*, 250.
(24) Meroueh, S. O.; Fisher, J. F.; Schlegel, H. B.; Mobashery, S. *J. Am. Chem. Soc.* **2005**, *127*, 15397.
(25) Oefner, C.; D'Arcy, A.; Daly, J. J.; Gubernator, K.; Charnas, R. L.; Heinze, I.; Hubschwerlen, C.; Winkler, F. K. *Nature* **1990**, *343*, 284.
(26) Kato-Toma, Y.; Ishiguro, M. *Bioorg. Med. Chem. Lett.* **2001**, *11*, 1161.
(27) Kato-Toma, Y.; Iwashita, T.; Masuda, K.; Oyama, Y.; Ishiguro, M. *Biochem. J.* **2003**, *371*, 175.
(28) Chen, Y.; Minasov, G.; Roth, T. A.; Prati, F.; Shoichet, B. K. *J. Am. Chem. Soc.* **2006**, *128*, 2970.
(29) Gao, X.; Xie, X. K.; Pashkov, I.; Sawaya, M. R.; Laidman, J.; Zhang, W. J.; Cacho, R.; Yeates, T. O.; Tang, Y. *Chem. Biol* **2009**, *16*, 1064.